HIGH VOLTAGE ELECTRON MICROSCOPY OF IGNEOUS ROCKS FROM APOLLO 15 AND 16

G.L.Nord°, J.S.Lally*, J.M.Christie+, A.H.Heuer°, R.M.Fisher*, D.T.Griggs+ and S.V.Radcliffe°
°Case Western Reserve University, Cleveland O.; *U.S.Steel Research Center, Monroeville, Pa.; +University of California, Los Angeles, Calif.

A suite of Apollo 15 and 16 igneous rocks -- 15555,163 and 15557,36 (Station 9(a), Hadley Rille), 60335,37 (Station 10), 62295,32 (Station 2) and 68415,76 (Station 8) -- have been examined by optical petrography, microprobe analysis and high voltage (1 MEV) transmission electron microscopy. The main emphasis of our studies has been directed to using the different substructural features resulting from exsolution and phase transformations, principally in clinopyroxenes and plagioclase, and from deformation and growth mistakes (dislocations, twins and stacking faults) in these phases and also olivine and orthopyroxene to deduce thermal and mechanical histories.

OPTICAL CHARACTERISTICS: Our thin sections of 15555,163 and 15557,36 (fine and coarse-grained olivine basalts) have been described previously (1) and do not differ significantly from thin sections described by other investigators (2). The two Apollo 15 rocks are mare pyroxene-rich basalts while our Apollo 16 samples (Type III rocks, Apollo 16 PET Report) are plagioclase-rich feldspathic basalts and a troctolite. Sample 60335,37 contains 1-2 mm blocky plagioclase (10%), possibly xenocrysts, several with patchy extinction; 0.5-1mm xenoliths (20%) of fine-grained (<0.05mm) plagioclase and larger (0.1mm) poikilitic clinopyroxene; skeletial ilmenite; troilite and iron. The xenoliths texturally range from diabasic to hornfelsic and the majority are completely holocrystalline. The groundmass (~70%) is diabasic; 60% is lath-shaped plagioclase, 20% anhedral olivines, and 15% poikilitic clinopyroxene, which also penetrates some xenoliths. The olivine is sometimes rimmed by pyroxene. A glassy mesostasis with abundant fine opaques fills interstices. Sample 62295,32 is a spinel-bearing troctolite with 0.1 to 0.4mm plagioclase laths and anhedral to subhedral olivines. Almost every olivine contains tubular or irregular silicate melt inclusions averaging 20μm. An oval 2mm dia. plagioclase xenocryst has a filled fracture of olivine. 10μm size octahedral spinels are found within the xenocryst in a 100μm wide zone adjacent only to the enclosing matrix. The spinels are abundant in the plagioclase and less so in the olivine of the groundmass. Another 1mm size xenolith contains both deformed and undeformed plagioclase fragments in a plagioclase, pyroxene matrix. A few spinel octahedra occur in the xenolith, but again only at the very edge. Sample 68415,76 is a plagioclase-rich intersertal basalt with 80% plagioclase, 10% clinopyroxene, 8% olivine, 1% opaques and 1% mesostasis. Several 1mm size plagioclase grains were probed, the compositions ranging from An_{97} in the core to An_{85} rims. One grain had a narrow 40 micron rim of An_{75}. Plagioclase compositions in a 1mm size cognate inclusion ranged from An_{91} to An_{95}.

ELECTRON MICROSCOPY: Both exsolution and domain structures in plagioclase and pyroxene vary in scale with composition. Correlation of scale with cooling rates requires an improved understanding of such composition dependence, a point which has been given particular attention here. The nature

HVEM OF APOLLO 15 AND 16

Nord, G. L., et al

of the effects are illustrated in the following. In 15555,163 the core region of a zoned pigeonite show fine scale (100Å) exsolution (tweed-texture) on (001) and (100) and occasional coarse (1200Å) augite plates at large separations (~1mm) with an adjacent depleted zone. As the edge of the pigeonite is approached, the exsolution coarsens and separate areas of (100) and (001) lamellae are found (Fig.1). These observed variations in scale can be attributed to the fact that the composition of the pigeonite core is such as to intersect the solvus at relatively low temperature (the solvus limb), while the more augitic rim exsolves at higher temperature near the solvus peak. In the case of antiphase domain structures (APD's), Figure 1 shows for this same zoned pigeonite the importance of the nucleation process in determining the domain size achieved. Heterogeneous nucleation is seen to occur with respect to augite exsolution lamellae by the large APD's adjacent to them (the smallest nucleate homogeneously away from them). Likewise, exsolution on (001) is coarser at the stacking faults (Fig.2). Again, in the anorthite core of a zoned plagioclase (An_{97}-An_{74}) from 68415,76 "c" domains vary in size from 1500Å (Fig.3a) to 300Å (Fig.3b) as the composition changes from An_{97} to An_{94}, and are either invisibly small or absent for lower anorthite contents. (The 1500Å size "c" domains found in the An_{97} region compared with the 5000Å domain size in 15415 (An_{97}) suggest that 15415 cooled more slowly than 68415.) Approaching the plagioclase rim, "b" domains ~1000Å in size suddenly appear, and there is a region several tens of microns wide between the core and rim in which neither "b" or "c" domains exist. Type "b" domains in the plagioclases of the cognate inclusions are quite variable morphologically and show good evidence of heterogeneous nucleation on a variety of pre-existing planar defects. For example, Figure 4 illustrates "b" domains which nucleated on a twin boundary and grew rapidly to form elongated rather than equidimensional domains (1). As "c" domains are much less influenced by pre-existing structures, they can be used with more confidence to estimate cooling rates - providing anorthite contents are known, since again both types vary in size with composition (1).

In samples 60335 and 62295, only results of the initial examination of the general characteristics of the major phases are available currently. In 60335 clinopyroxene exhibits exsolution on (001) major, (100) minor and there are large APD's in the pigeonite phase. Both the pyroxene and plagioclase are free of deformation. In 62295, the matrix olivine exhibits rare dislocation arrays, but contains inclusions of glass and particles (Fig.5). The mesostasis (Fig.6) is complex and contain glass, some crystalline material, and occasionally a radiating aggregate of highly twinned plagioclase. The fine 1μm groundmass of an included breccia fragment shows recrystallization of plagioclase into an annealed polycrystalline matrix with occasional (~300Å) pores (possibly gas-filled). Fine "c" domains were imaged in the highly twinned, non-recrystallized plagioclase of the xenolith, but it is not known if domain structures are present in the recrystallized plagioclase. Further examination of these and additional samples are in progress.

1. Heuer et al. (1972) in The Apollo Lunar Samples (ed. Chamberlain and Watkins) Lunar Science Institute, Houston, page 98-102.
2. Brown et al. (1972) in Proc. Third Lunar Sci. Conf. (ed. E.A.King),

HVEM OF APOLLO 15 AND 16

Nord, G.L. et al

The MIT Press, Cambridge, Mass., Vol. 1, page 401-422.

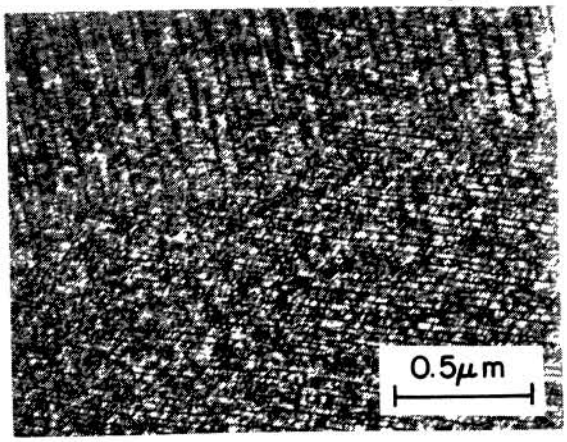

Fig.1 Fine (001) and (100) augite-pigeonite (in APB contrast) lamellae 15555.

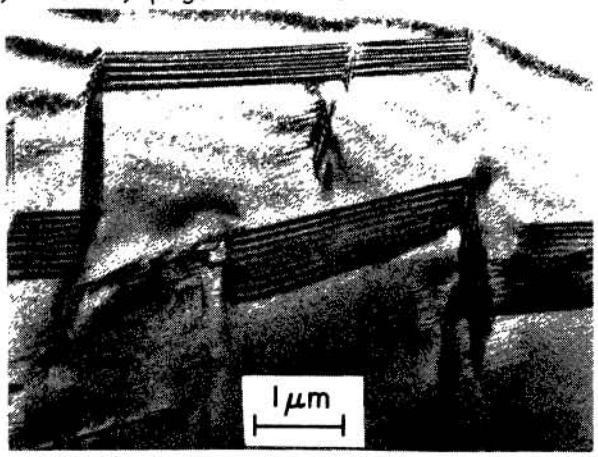

Fig.2 Enhanced exsolution on stacking faults in pigeonite 15555.

Courtesy MIT Press.

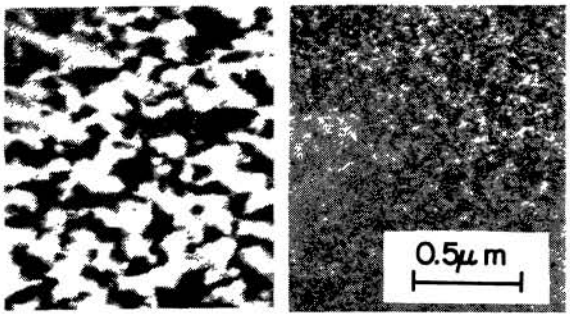

Fig.3a,b "c" domains in An_{97} and An_{94} 68415.

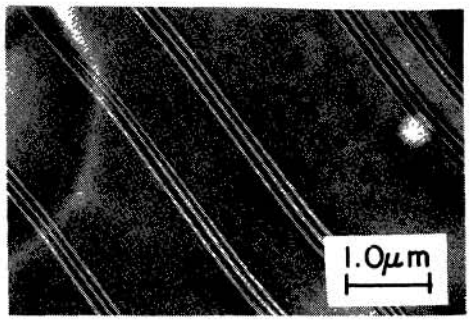

Fig.4 Lamellar "b" domains in 68415.

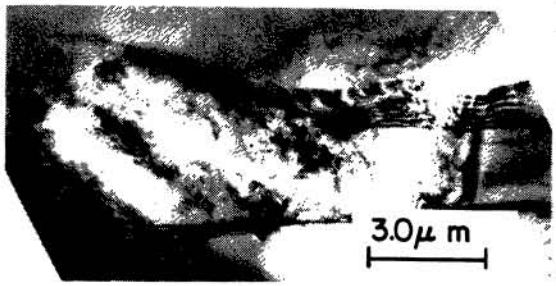

Fig.5 Crystal-glass inclusion in olivine 62295.

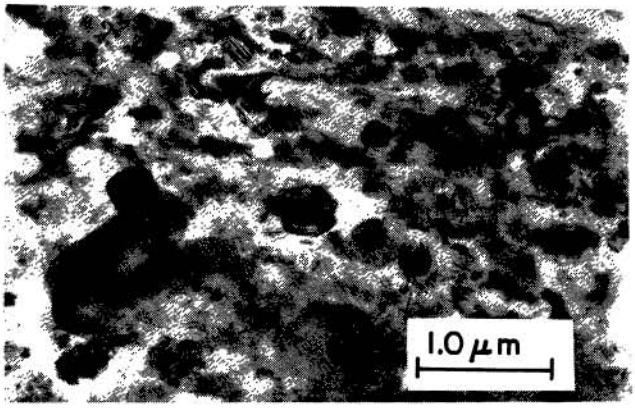

Fig.6 Mesostasis in 62295.